

## Activation of N<sub>2</sub>O and SO<sub>2</sub> by the P–B Bond System. Reversible Binding of SO<sub>2</sub> by the P–O–B Geminal Frustrated Lewis Pair

Natalia Szykiewicz, Jarosław Chojnacki, and Rafał Grubba\*

Cite This: *Inorg. Chem.* 2020, 59, 6332–6337

Read Online

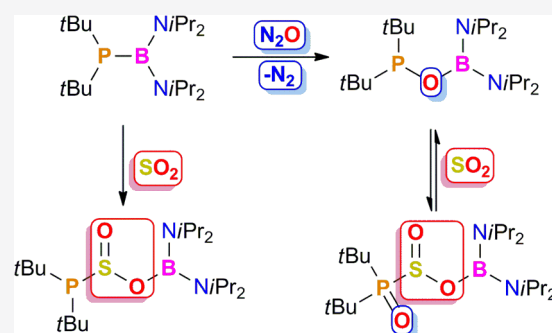
ACCESS |

Metrics & More

Article Recommendations

Supporting Information

**ABSTRACT:** Herein, we present the first transformation of borylphosphine into borylphosphinite using nitrous oxide. Borylphosphine reacts with N<sub>2</sub>O via insertion of a single oxygen atom into the P–B bond and formation of a P–O–B bond system. Borylphosphine and borylphosphinite capture SO<sub>2</sub> and activate it in an irreversible and reversible manner, respectively.



### 1. INTRODUCTION

Metal-free catalysis based on systems that mimic the reactivity of transition metal compounds toward hydrogen and greenhouse gases is currently one of the most widely studied fields of main-group element chemistry.<sup>1,2</sup> We are searching for compounds that not only capture small molecules but also enable their clean and efficient conversion into complex organic derivatives or their decomposition into more environmentally friendly species. The challenge is to develop agents capable of fixing highly reactive molecules such as SO<sub>2</sub> with the formation of selected products as well as activating species that kinetically or thermodynamically reluctant to decompose and be reduced, such as N<sub>2</sub>O or CO<sub>2</sub>, without employing harsh reaction conditions.

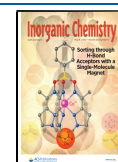
Despite its high oxidation potential, N<sub>2</sub>O is kinetically inert, and only highly oxophilic compounds are known to react with N<sub>2</sub>O under mild conditions.<sup>3</sup> Thus, these reactions are extremely selective and proceed via oxygen atom transfer and release of N<sub>2</sub>. The covalent capture of N<sub>2</sub>O may be achieved by frustrated Lewis pairs (FLPs)<sup>4–6</sup> or N-heterocyclic carbenes (NHCs),<sup>7,8</sup> leading to the formation of stable adducts involving an intact N<sub>2</sub>O moiety: R<sub>3</sub>PNNOR<sub>3</sub> or NHC–NNO, respectively. Upon thermal or photochemical activation, these adducts decompose and liberate dinitrogen, giving R<sub>3</sub>P(O)BR<sub>3</sub> or the corresponding urea. Although in NHC–(N<sub>2</sub>O), the C–N bond is relatively strong, phosphorus is prone to oxidation, and zwitterionic R<sub>3</sub>P(N<sub>2</sub>O)BR<sub>3</sub> compounds are “kinetically trapped” due to the presence of the highly electrophilic borane. The product is stable only when the Lewis acid is sufficiently strong and coordination of borane to the oxygen atom is faster than phosphine oxidation.<sup>4,5,9</sup>

Unlike N<sub>2</sub>O, SO<sub>2</sub> is a toxic and a more reactive Lewis acidic molecule that is considered a S-containing feedstock for chemicals. SO<sub>2</sub> reacts with a wide range of organic species, typically as an oxidizing agent, and forms stable adducts with amines, of which solid adducts are utilized as easily handled sulfur dioxide surrogates in organic syntheses.<sup>10</sup> While nitrogen base–SO<sub>2</sub> adducts are well characterized, reaction with phosphines results in the formation of phosphine oxides and phosphine sulfides in a 2:1 ratio.<sup>11</sup> Very recently, Dielmann et al. isolated the first phosphine–SO<sub>2</sub> adducts.<sup>12</sup> The slow decomposition of these compounds helped to elucidate the mechanism of their oxidation: nucleophilic attack by the phosphine at the sulfur atom of SO<sub>2</sub> followed by the formation of a P–O bond with elimination of SO.<sup>12</sup> Phosphine–SO<sub>2</sub> adducts may be stabilized in the presence of Lewis acids, for instance, by using FLPs. Inter- and intramolecular FLPs bind SO<sub>2</sub>, yielding the corresponding R<sub>3</sub>P/N–S(O)–O–B/SiR<sub>3</sub> as a linear or cyclic zwitterions upon formation of P–S (or N–S) and B–O (or Si–O and Al–O) bonds, respectively.<sup>13–15</sup> Unlike FLPs, stable boryl(phosphino)carbene was found not only to capture but also to activate the SO<sub>2</sub> molecule in an unprecedented manner, giving sulfine derivatives R<sub>2</sub>P(O)–C(SO)–BR<sub>2</sub>.<sup>16</sup>

Our group has a research interest in the synthesis and reactivity of low-valent P,B-based systems<sup>17–20</sup> with applica-

Received: February 12, 2020

Published: April 14, 2020

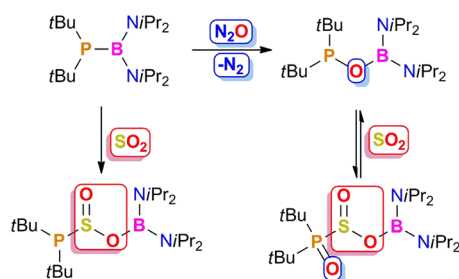


tions in the activation of small inorganic molecules. We pay special attention to amino-substituted phosphinoboranes<sup>19</sup> and diphosphinoboranes,<sup>20</sup> borylphosphine-like species containing a very long single P–B bond with a pyramidal P atom and a planar B atom.<sup>21</sup> As a continuation of our studies, we decided to explore the reactivity of these species toward inert N<sub>2</sub>O and highly reactive SO<sub>2</sub>. From a series of monomeric diamino-phosphinoboranes recently synthesized by us, we tested the reactivity of *t*Bu<sub>2</sub>P–B(NiPr<sub>2</sub>)<sub>2</sub> (**1**)<sup>19</sup> due to its high nucleophilicity and the presence of *t*Bu and NiPr<sub>2</sub> substituents, which should promote the crystallization of activation products.

## 2. RESULTS AND DISCUSSION

The reaction of a toluene solution of **1** with N<sub>2</sub>O (1 atm) at room temperature led to complete conversion of the parent P–B compound into borylphosphinite **2** after 24 h (Scheme 1). Furthermore, during the reaction, vigorous gas evolution was observed.

### Scheme 1. Reaction of **1** with Nitrous Oxide and Reactions of **1** and **2** with Sulfur Dioxide



The <sup>31</sup>P{<sup>1</sup>H} NMR spectrum of the reaction mixture displays a singlet at 144.7 ppm, which is strongly shifted downfield in comparison to the resonance of parent **1** (−8.0 ppm). Moreover, contrary to the spectrum of **1**, in which a broad signal was observed, the corresponding spectrum of **2** shows a sharp resonance, indicating the loss of direct phosphorus–boron coupling. Notably, the <sup>31</sup>P{<sup>1</sup>H} chemical shift of **2** is in the typical region for phosphinites (e.g., for *i*Pr<sub>2</sub>POPh, 149 ppm). These spectral data indicated that newly formed **2** possesses a *t*Bu<sub>2</sub>PO phosphinite moiety. The <sup>11</sup>B NMR spectrum of **2** shows a singlet at 26.7 ppm, which is shifted upfield in comparison to the corresponding signal of **1** (39.5 ppm) and has a typical value for tricoordinated boron compounds with N-donor ligands.<sup>19,20,22</sup> Analytically pure **2** was quantitatively obtained by solvent evaporation as an air-stable, white crystalline solid (94% yield). Crystals of **2** suitable for X-ray analysis were formed from a concentrated petroleum ether solution at −80 °C. X-ray structure determination unambiguously confirmed the identity of **2** and showed that a single oxygen atom was inserted into the P–B bond (Figure 1).

The boron and both nitrogen atoms exhibit trigonal planar geometry, whereas the phosphorus atom is pyramidal. The N1–B1 [1.465(1) Å], N2–B1 [1.424(2) Å], and B1–O2 [1.413(1) Å] bond distances are significantly shorter than the corresponding single covalent bonds (sum of the single-covalent bond radii for B and N, 1.56 Å; that for B and O, 1.48 Å),<sup>23</sup> which suggests substantial  $\pi$ -donor interactions between N and O atoms with a boron center. The P1–O1 distance of

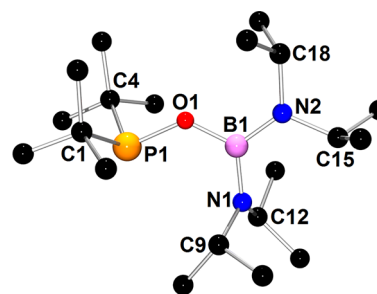


**Figure 1.** X-ray structure of **2** showing the atom numbering scheme. The H atoms have been omitted for the sake of clarity.

1.6582(9) Å is similar to those observed for compounds with phosphinite moieties attached to boryl groups.<sup>22,24,25</sup> The P–O–B angle is 126.51(7)°. Interestingly, P, O, B, and both N atoms lie in almost the same plane. This striking structural feature of **2** can be explained on the basis of NBO analysis. The O1 and B1 atoms display sp<sup>2</sup> hybridization; furthermore, the unhybridized p lone pair on the O1 atom interacts with the B1 atom, resulting in  $\pi$ -bonding. Additionally, significant donor–acceptor interactions were also observed between the nitrogen atoms and the B1 atom. Notably, there is no significant interaction between the P1 atom and the B1 center.

According to calculations of nucleophilic ( $f_N$ ) and electrophilic ( $f_E$ ) Fukui functions, in **2**, both P and B atoms are neutral with values of  $f_N$  and  $f_E$ , respectively, close to zero. The nucleophilic properties of phosphorus decreased in comparison to those of parent **1** ( $f_N = 0.277$ ), while the electrophilicity of the boron atom remained unchanged.

We did not observe the formation of adduct **1** with N<sub>2</sub>O containing a PNNOB structural motif similar to those obtained in reactions involving P- and B-based FLPs and N<sub>2</sub>O.<sup>4,5</sup> Considering that the Lewis acidic properties of the B center in **1** are quenched due to strong  $\pi$ -donation from N atoms,<sup>19</sup> we assume that coordination of the terminal O atom of the N<sub>2</sub>O molecule to B is very weak and that oxidation of the *t*Bu<sub>2</sub>P phosphanyl group is favored. Consequently, oxidation of **1** by N<sub>2</sub>O leads to the formation of **2** bearing a P–O–B skeleton with simultaneous liberation of N<sub>2</sub>. Insertion of a single oxygen atom into a single covalent bond is very rare<sup>22,26,27</sup> except in biological systems utilizing monooxygenases.<sup>28</sup> The insertion of an oxygen atom into a P–B bond was observed for the first time by Nöth and Schrägle in the reaction of Et<sub>2</sub>P–B(NMe<sub>2</sub>)<sub>2</sub> with O<sub>2</sub>, which gave Et<sub>2</sub>P(=O)–O–B(NMe<sub>2</sub>)<sub>2</sub>.<sup>29</sup> An alternative method was proposed by Pringle and co-workers. Therein, Me<sub>3</sub>NO was used as an oxidizing agent that enables the insertion of the single O atom to form P–O–B species.<sup>22</sup> The presented reaction of **1** with N<sub>2</sub>O constitutes a simple and effective method of synthesizing borylphosphinites, an emerging class of compounds with applications in the activation of small molecules<sup>24,25</sup> and the synthesis of transition metal catalysts.<sup>22</sup>

Next, we tested the reactivity of **1** toward the electrophilic SO<sub>2</sub> molecule [ $f_E(\text{SO}_2) = 0.525$ ]. The reaction of **1** with gaseous SO<sub>2</sub> (1 atm) in toluene was performed at room temperature for 5 min. After evaporation of the solvent-pure product, **3** was isolated quantitatively as a yellowish solid (98% yield) (Scheme 1). X-ray-quality crystals of **3** were obtained from a saturated petroleum ether solution at −20 °C. <sup>31</sup>P{<sup>1</sup>H} NMR spectroscopy reveals that the reaction of **1** with SO<sub>2</sub> is very clean, with **3** as the only main product. The <sup>31</sup>P{<sup>1</sup>H}

spectrum of **3** shows a downfield-shifted sharp singlet at 111.4 ppm. The  $^{11}\text{B}$  spectrum of **3** displays a resonance at 26.4 ppm with almost the same value of the chemical shift as observed for **2**, indicating the same coordination environment of the B atom in both **2** and **3**. X-ray structural analysis of **3** confirms that the aforementioned reaction proceeds via insertion of the  $\text{SO}_2$  molecule into a single P–B bond (Figure 2).

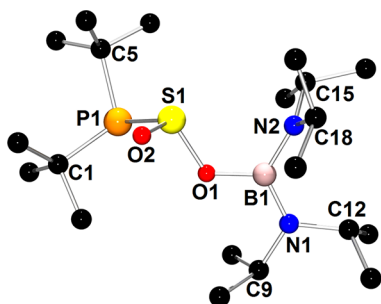


**Figure 2.** X-ray structure of **3** showing the atom numbering scheme. The H atoms have been omitted for the sake of clarity. One molecule of the two present in the asymmetric unit was selected.

The pyramidal geometry around the P1 atom and planar geometries around B1 at the N1 and N2 atoms are clearly visible. The geometry at S1 is pyramidal due to the presence of a lone pair of electrons. Similar to those in **2**, in **3**, the O1–B1 [1.426(2) Å], N1–B1 [1.402(2) Å], and N2–B1 [1.453(2) Å] distances are significantly shorter than typical single covalent bonds, indicating  $\pi$ -interactions with the boron center. The P1–S1 [2.2176(7) Å] and S1–O1 [1.634(1) Å] bond lengths are very close to the expected distances for the corresponding single covalent bonds (sum of the single covalent bond radii for P and S, 2.14 Å; that for S and O, 1.66 Å),<sup>23</sup> whereas the S1–O2 [1.476(1) Å] distance is typical for a S=O bond (sum of the double covalent bond radii for S and O, 1.51 Å).<sup>30</sup> Due to  $\text{sp}^2$  hybridization of the O1 and B1 atoms, S1, O1, B1, and N1 are almost coplanar. Moreover, the value of the B1–O1–S1 angle [118.74(8)°] indicates  $\text{sp}^2$  hybridization of the O1 atom.

Notably, the insertion of  $\text{SO}_2$  into the P–B bond is irreversible. Solid **3** is stable under vacuum and does not regenerate parent **1**. In contrast to **2**, compound **3** is prone to hydrolysis and must be handled under an inert atmosphere.

According to the Gibbs free energy profile, insertion of the  $\text{SO}_2$  molecule into the P–B bond proceeds via a two-step mechanism analogous to the one we have recently elucidated for the reaction of **1** with  $\text{CO}_2$ <sup>19</sup> (see the Supporting Information for details). In the first step, the phosphorus atom binds with the sulfur atom, resulting in intermediate **1**- $\text{SO}_2$  adduct **I** (Figure S23). The second, rate-determining step proceeds via a transition state with a four-membered PSOB ring. The simultaneous formation of B–O and cleavage of the P–B bond give final product **3**. The formation of **3** is thermodynamically favored, with a free energy value ( $\Delta G^\circ_{298}$ ) of  $-33.7$  kcal/mol, and more energetically favored than the corresponding insertion of a  $\text{CO}_2$  molecule ( $-20.1$  kcal/mol).<sup>19</sup> Moreover, as the linear  $\text{CO}_2$  molecule has to bend during fixation and is less electrophilic than  $\text{SO}_2$ , the energy barrier  $\Delta G^\ddagger$  of 14.4 kcal/mol for the formation of **3** is significantly lower than  $\Delta G^\ddagger$  for the reaction of **1** with  $\text{CO}_2$  (27.3 kcal/mol).<sup>19</sup>

Compound **2** can be considered as geminal phosphinoborane in which the phosphanyl and boryl groups are separated by a single oxygen atom. Geminal methylene- or oxygen-bridged phosphinoboranes are preorganized FLPs with intramolecular donor and acceptor sites oriented in the same direction for optimal interaction with the substrate.<sup>24,25,31,32</sup> Intramolecular self-quenching of Lewis acid and base centers is not observed, as the formation of strained three-membered PCB or POB rings is not thermodynamically favored.<sup>24,31</sup> Despite the mild Lewis acidity of the boron center, methylene-bridged geminal FLPs bind and/or activate, e.g.,  $\text{H}_2$ ,  $\text{CO}_2$ , or  $\text{SO}_2$ ,<sup>31,32</sup> while oxygen-bridged ones bind and/or activate, e.g.,  $\text{CO}_2$  or  $\text{CS}_2$ .<sup>24,25</sup> The interesting structural features of **2** and recent advances in the chemistry of geminal FLPs encourage us to study the reactivity of **2** toward small inorganic molecules. We performed reactions of **2** with a series of inorganic gases:  $\text{H}_2$ ,  $\text{CO}_2$ , and  $\text{SO}_2$ . All of these reactions were carried out under the same mild conditions: toluene as the solvent, room temperature, and 1 atm pressure of the gaseous reagent. We did not detect the formation of any products in the case of reactions involving  $\text{H}_2$  and  $\text{CO}_2$ . In contrast, borylphosphinite **2** reacted rapidly with  $\text{SO}_2$  (Scheme 1).  $^{31}\text{P}\{\text{H}\}$  NMR spectroscopic analysis of the reaction mixture showed the appearance of a new sharp singlet at 81.0 ppm, which is significantly shifted to a lower frequency compared to that of borylphosphinite **2** (144.7 ppm). Otherwise, the  $^{11}\text{B}$  NMR spectra of the reaction solution consist of only one signal at 27.0 ppm with a chemical shift very similar to those observed for **2** (26.7 ppm). Complete conversion of **2** to new product **4** is observed after a few minutes, and no other products are present in the reaction mixture. Cooling the reaction mixture to  $-80$  °C yielded yellow crystals, which were characterized as  $t\text{Bu}_2\text{P}(=\text{O})\text{-S}(=\text{O})\text{-O-B}(\text{NiPr}_2)_2$  (**4**) on the basis of NMR spectroscopy and X-ray structural analyses. The molecular structure of **4** is presented in Figure 3.

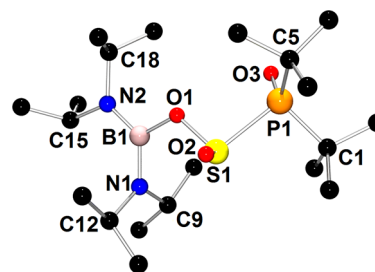


**Figure 3.** X-ray structure of **4** showing the atom numbering scheme. The H atoms have been omitted for the sake of clarity.

The phosphinyl  $t\text{Bu}_2\text{P}(=\text{O})$  group is linked to the  $(i\text{Pr}_2\text{N})\text{B}$  boryl group via the  $\text{SO}_2$  moiety. In comparison to **2**, **4** retains planar geometries around the B1, N1, and N2 atoms. The geometry and metric parameters of the P1–S1(O2)–O1–B1 skeleton in **4** resemble those observed for the analogous structural motif in compound **3**. The S1=O2 and P1=O3 bonds are *anti*-oriented to each other, and the O2–S1–P1–O3 torsion angle is  $-142.01(8)^\circ$ .

Additionally, we investigated whether compound **4** could transform into a hypothetical tautomer with the formula  $t\text{Bu}_2\text{P-O-S}(=\text{O})\text{-O-B}(i\text{Pr}_2\text{N})_2$  (**4'**). To this end, we modeled and optimized the structure of tautomer **4'** using DFT methods (see Figure S38). By calculating the free energy value, we found that transformation of **4** into **4'** is not



thermodynamically favored with a  $\Delta G^\circ_{298}$  of 4.3 kcal/mol (Figure S25), which indicates that tautomer **4** is preferred both in the solid state and in solution.

Interestingly, **2** reacts with  $\text{SO}_2$  during the formation of **4** in a reversible manner. Without an  $\text{SO}_2$  atmosphere, compound **4** slowly decomposed at room temperature both in the solid state and in solution into starting borylphosphinite **2**. The gentle heating of solid **4** under vacuum up to 35 °C for 2 h leads to complete regeneration of **2** (Figure S19).

To the best of our knowledge, the reaction of **2** with  $\text{SO}_2$  is the first example of a reversible activation of the  $\text{SO}_2$  molecule by a P-based system. The combinations of strong Lewis basic phosphines with strong Lewis acidic boranes form irreversibly stable zwitterionic adducts with  $\text{SO}_2$  due to strong P–S and B–O interactions.<sup>13,15</sup> Recently, the first stable adducts of highly nucleophilic phosphines and  $\text{SO}_2$  were isolated, but they decompose at room or elevated temperatures to  $\text{R}_3\text{P}=\text{O}$ ,  $\text{R}_3\text{P}=\text{S}$ , and  $\text{SO}$ .<sup>12</sup> The product of activation of  $\text{SO}_2$  by boryl(phosphino)carbene decomposes above –25 °C to uncharacterized compounds.<sup>16</sup> The reaction of **2** with  $\text{SO}_2$  can be formally seen as the insertion of  $\text{SO}_2$  into the P–B bond of the hypothetical tautomer of  $t\text{Bu}_2\text{P}-\text{O}-\text{B}(\text{NiPr}_2)_2$  (**2**) with the formula  $t\text{Bu}_2\text{P}(=\text{O})-\text{B}(\text{NiPr}_2)_2$ . If we replace the boryl group with H, it resembles a well-known tautomerism of phosphinous acid [ $\text{R}_2\text{P}-\text{O}-\text{H}$  vs  $\text{R}_2\text{P}(=\text{O})-\text{H}$ ].<sup>33,34</sup> In this context, the reaction of **2** cannot be treated as analogous to the oxidation of phosphine by  $\text{SO}_2$ .

On the grounds of DFT calculations, we proposed a reaction mechanism that supports this statement (Figure 4). Despite

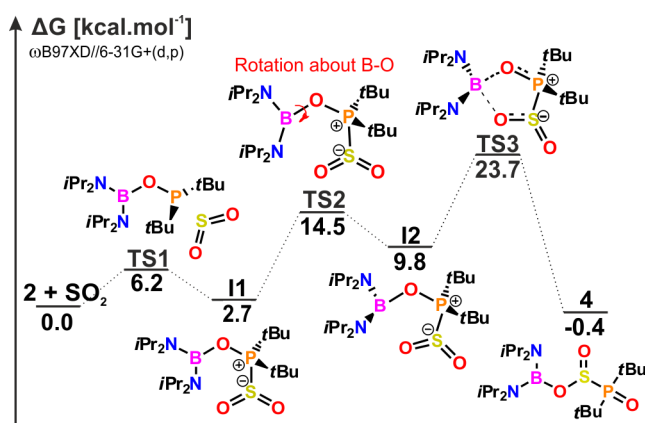


Figure 4. Gibbs free energy profile of the reaction of **2** with  $\text{SO}_2$ .

the neutral character of phosphorus ( $f_N = 0.008$  for **2** in comparison to a value of 0.277 for **1**), the reaction starts with an electrophilic attack by the  $\text{SO}_2$  molecule on the P lone pair, giving intermediate **I1**. Via rotation about the B–O bond, the 2- $\text{SO}_2$  adduct adopts a conformation that enables the interaction of boron and the OSO oxygen atom (**I2**). It leads to simultaneous formation of B–OSO and cleavage of the B–OP bond with migration of the linking B–O–P oxygen atom to phosphorus via five-membered OBOPS transition state **TS3**. The resulting product **4** is formed reversibly, and in the absence of an  $\text{SO}_2$  atmosphere, an equilibrium is established between parent **2** and **4**, which is justified by the calculated value of free energy  $\Delta G^\circ_{298}$  of –0.4 kcal/mol.

### 3. CONCLUSIONS

Despite the low Lewis acidity of the boron center in the diamino-phosphinoboranes, these compounds were successfully applied in the activation of small inorganic molecules. The phosphinoborane **1** containing direct P–B bond reacts with  $\text{N}_2\text{O}$ , leading to insertion of an oxygen atom into the P–B bond and formation of geminal P–O–B phosphinoborane **2**. Moreover, we compared the reactivity of phosphinoboranes (P–B) and geminal phosphinoboranes (P–O–B) toward  $\text{SO}_2$ . Our studies revealed that both systems capture and activate the  $\text{SO}_2$  molecule in irreversible and reversible manners, respectively. The presented reactions constitute new synthetic methods for insertion of a single oxygen atom into the P–B bond and an unprecedented example of reversible activation of  $\text{SO}_2$  by a P-based compound. As a continuation of this work, we are currently studying reactions of diphosphinoboranes possessing two P–B bonds with small molecules and these results will be published in due course.

### 4. EXPERIMENTAL SECTION

**General Information.** All manipulations were carried out under a dry argon atmosphere by using flame-dried Schlenk-type glassware on a vacuum line or in a glovebox. Solvents were dried by standard procedures over Na(K)/K/Na/benzophenone and distilled under argon. One-dimensional ( $^{31}\text{P}$ ,  $^{13}\text{C}$ ,  $^{11}\text{B}$ , and  $^1\text{H}$ ) and two-dimensional NMR spectra in a  $\text{C}_6\text{D}_6$  or toluene- $d_8$  solution were recorded on a Bruker AV400 MHz spectrometer (external standard TMS for  $^1\text{H}$  and  $^{13}\text{C}$ ; 85%  $\text{H}_3\text{PO}_4$  for  $^{31}\text{P}$ ) at ambient temperature. Reaction progress was monitored by  $^{31}\text{P}\{^1\text{H}\}$  and  $^{11}\text{B}$  NMR spectra of reaction mixtures. The FTIR spectra of crystalline products were recorded using a Nicolet iS50 FT-IR spectrometer equipped with the Specac Quest single-reflection diamond attenuated total reflectance (ATR) accessory, and spectral analysis was carried out by using the OMNIC software package. Elemental analyses were performed at the University of Gdańsk using a Vario El Cube CHNS apparatus. Crystallographic analyses were performed on a STOE IPDS II diffractometer using Mo  $K\alpha$  radiation ( $\lambda = 0.71073$  Å). Phosphinoborane **1** was synthesized via the procedure described in ref 19.

**Preparation of 2.** A solution of **1** (178 mg, 0.5 mmol) in toluene (3 mL) was slowly frozen in a liquid nitrogen bath, evacuated to 0.01 Torr, and backfilled with  $\text{N}_2\text{O}$  (1 atm). The solution was allowed to warm to room temperature and stirred for 24 h.  $^{31}\text{P}\{^1\text{H}\}$  NMR of the colorless reaction mixture revealed a complete conversion of **1** into **2**. The solvent was evaporated, and the residue was dried under vacuum (0.01 Torr) giving **2** as a white, crystalline solid: yield 94% (175 mg, 0.470 mmol). The solid was dissolved in 1  $\text{cm}^3$  of petroleum ether and left at –80 °C to afford colorless, X-ray-quality crystals of **2** that were dried in vacuum: yield 65% (120 mg, 0.322 mmol);  $^{31}\text{P}\{^1\text{H}\}$  NMR ( $\text{C}_6\text{D}_6$ )  $\delta$  144.7 (s);  $^{11}\text{B}$  NMR ( $\text{C}_6\text{D}_6$ )  $\delta$  26.7 (s);  $^1\text{H}$  NMR ( $\text{C}_6\text{D}_6$ )  $\delta$  3.68 (sept,  $^3J_{\text{HH}} = 6.8$  Hz, 2H, CH), 3.68 (sept,  $^3J_{\text{HH}} = 6.8$  Hz, 2H, CH), 1.27 (d,  $^3J_{\text{HH}} = 6.8$  Hz, 24H,  $\text{CHCH}_3$ ), 1.23 (d,  $^3J_{\text{PH}} = 10.8$  Hz, 18H,  $\text{CCH}_3$ );  $^{13}\text{C}\{^1\text{H}\}$  NMR ( $\text{C}_6\text{D}_6$ )  $\delta$  46.5 (s,  $\text{CHCH}_3$ ), 46.5 (s,  $\text{CHCH}_3$ ), 35.0 [d,  $^1J_{\text{PC}} = 31.8$  Hz,  $\text{C}(\text{CH}_3)_3$ ], 28.3 [d,  $^2J_{\text{PC}} = 16.3$  Hz,  $\text{C}(\text{CH}_3)_3$ ], 24.3 (s,  $\text{CHCH}_3$ ); IR (solid)  $\nu$  2960, 2863, 1469, 1431, 1363, 1295, 1238, 1189, 1151, 1115, 1020, 1007, 996, 876, 805, 787, 751  $\text{cm}^{-1}$ . Elemental analysis. Calcd for  $\text{C}_{20}\text{H}_{46}\text{BN}_2\text{O}_2\text{P}$ : C, 64.51; H, 12.45; N, 7.52. Found: C, 64.24; H, 12.32; N, 7.42.

**Preparation of 3.** A solution of **1** (178 mg, 0.5 mmol) in toluene (3 mL) was slowly frozen in a liquid nitrogen bath, evacuated to 0.01 Torr, and backfilled with  $\text{SO}_2$  (1 atm). The solution was allowed to warm to room temperature and stirred for 5 min.  $^{31}\text{P}\{^1\text{H}\}$  NMR of the yellow reaction mixture revealed a complete conversion of **1** to **3**. The solvent was evaporated, and the residue was dried under vacuum (0.01 Torr), giving **3** as a yellowish solid: yield 98% (205 mg, 0.488 mmol). The solid was dissolved in 1  $\text{cm}^3$  of petroleum ether and left at –20 °C to afford colorless, and X-ray-quality crystals of **3** were

dried in vacuum. Yield of 75% (157 mg, 0.373 mmol). The compound **3** is thermally stable both in the toluene solution and in the solid state; it does not decompose upon being heating to 90 °C:  $^{31}\text{P}\{^1\text{H}\}$  NMR ( $\text{C}_6\text{D}_6$ )  $\delta$  111.4 (s);  $^{11}\text{B}$  NMR ( $\text{C}_6\text{D}_6$ )  $\delta$  26.4 (s);  $^1\text{H}$  NMR ( $\text{C}_6\text{D}_6$ )  $\delta$  3.42 (sept,  $^3J_{\text{HH}} = 6.6$  Hz, 4H, CH), 1.54 (d,  $^3J_{\text{PH}} = 11.6$  Hz, 9H,  $\text{CCH}_3$ ), 1.32 (d,  $^3J_{\text{PH}} = 10.8$  Hz, 9H,  $\text{CCH}_3$ ), 1.22 (d,  $^3J_{\text{HH}} = 6.6$  Hz, 12H,  $\text{CHCH}_3$ ), 1.21 (d,  $^3J_{\text{HH}} = 6.6$  Hz, 12H,  $\text{CHCH}_3$ );  $^{13}\text{C}\{^1\text{H}\}$  NMR ( $\text{C}_6\text{D}_6$ )  $\delta$  45.7 (s,  $\text{CHCH}_3$ ), 37.7 [d,  $^1J_{\text{PC}} = 40.9$  Hz,  $\text{C}(\text{CH}_3)_3$ ], 33.5 [d,  $^1J_{\text{PC}} = 30.0$  Hz,  $\text{C}(\text{CH}_3)_3$ ], 30.3 [d,  $^2J_{\text{PC}} = 12.7$  Hz,  $\text{C}(\text{CH}_3)_3$ ], 29.8 [d,  $^2J_{\text{PC}} = 12.7$  Hz,  $\text{C}(\text{CH}_3)_3$ ], 22.6 (s,  $\text{CHCH}_3$ ), 22.2 (s,  $\text{CHCH}_3$ ); IR (solid)  $\nu$  2957, 2866, 1471, 1382, 1362, 1309, 1250, 1180, 1152, 1076, 1009, 979, 868, 802, 735  $\text{cm}^{-1}$ . Elemental analysis. Calcd for  $\text{C}_{20}\text{H}_{46}\text{BN}_2\text{O}_2\text{PS}$ : C, 57.13; H, 11.03; N, 6.66; S, 7.63. Found: C, 56.92; H, 10.90; N, 6.62; S, 7.49.

**Preparation of 4.** A solution of **2** (198 mg, 0.5 mmol) in toluene (2 mL) was slowly frozen in a liquid nitrogen bath, evacuated to 0.01 Torr, and backfilled with  $\text{SO}_2$  (1 atm). The solution was allowed to warm to room temperature and stirred for 5 min.  $^{31}\text{P}\{^1\text{H}\}$  NMR of the yellow reaction mixture revealed a complete conversion of **2** to **4**. The X-ray-quality crystals were obtained from the  $\text{SO}_2$ -saturated toluene solution at  $-80$  °C. Compound **4** is stable only in the presence of  $\text{SO}_2$ . Removing of the solvent over the yellow crystals as well as the evaporation of the solvent after reaction results in slow decomposition into substrate **2**. Drying of **4** under vacuum in the oil bath at 35 °C for 2 h leads to complete regeneration of the substrate. The formation of **4** is reversible, and in the presence of  $\text{SO}_2$ , the product is yielded again:  $^{31}\text{P}\{^1\text{H}\}$  NMR ( $\text{C}_6\text{D}_6$ )  $\delta$  81.0 (s);  $^{11}\text{B}$  NMR ( $\text{C}_6\text{D}_6$ )  $\delta$  27.0 (s);  $^1\text{H}$  NMR ( $\text{C}_6\text{D}_6$ )  $\delta$  3.39 (sept,  $^3J_{\text{HH}} = 6.7$  Hz, 4H, CH), 1.49 (d,  $^3J_{\text{PH}} = 14.8$  Hz, 9H,  $\text{CCH}_3$ ), 1.29 (d,  $^3J_{\text{PH}} = 13.8$  Hz, 9H,  $\text{CCH}_3$ ), 1.23 (d,  $^3J_{\text{HH}} = 6.6$  Hz, 12H,  $\text{CHCH}_3$ ), 1.19 (d,  $^3J_{\text{HH}} = 6.6$  Hz, 12H,  $\text{CHCH}_3$ );  $^{13}\text{C}\{^1\text{H}\}$  NMR ( $\text{C}_6\text{D}_6$ )  $\delta$  45.7 (s,  $\text{CHCH}_3$ ), 41.3 [d,  $^1J_{\text{PC}} = 31.8$  Hz,  $\text{C}(\text{CH}_3)_3$ ], 37.8 [d,  $^1J_{\text{PC}} = 37.2$  Hz,  $\text{C}(\text{CH}_3)_3$ ], 27.4 [s,  $\text{C}(\text{CH}_3)_3$ ], 26.4 [s,  $\text{C}(\text{CH}_3)_3$ ], 22.2 (s,  $\text{CHCH}_3$ ), 21.8 (s,  $\text{CHCH}_3$ ); IR (solid)  $\nu$  2967, 2930, 2872, 1468, 1398, 1382, 1362, 1311, 1249, 1169, 1096, 1073, 1011, 974, 867, 804, 752  $\text{cm}^{-1}$ .

## ■ ASSOCIATED CONTENT

### Supporting Information

The Supporting Information is available free of charge at <https://pubs.acs.org/doi/10.1021/acs.inorgchem.0c00435>.

Crystallographic details, spectroscopic details, and computational details (PDF)

### Accession Codes

CCDC 1959420–1959422 contain the supplementary crystallographic data for this paper. These data can be obtained free of charge via [www.ccdc.cam.ac.uk/data\\_request/cif](http://www.ccdc.cam.ac.uk/data_request/cif), or by emailing [data\\_request@ccdc.cam.ac.uk](mailto:data_request@ccdc.cam.ac.uk), or by contacting The Cambridge Crystallographic Data Centre, 12 Union Road, Cambridge CB2 1EZ, UK; fax: +44 1223 336033.

## ■ AUTHOR INFORMATION

### Corresponding Author

Rafał Grubba – Department of Inorganic Chemistry, Faculty of Chemistry, Gdańsk University of Technology, 80-233 Gdańsk, Poland; [orcid.org/0000-0001-6965-2304](https://orcid.org/0000-0001-6965-2304); Email: [rafal.grubba@pg.edu.pl](mailto:rafal.grubba@pg.edu.pl)

### Authors

Natalia Szynekiewicz – Department of Inorganic Chemistry, Faculty of Chemistry, Gdańsk University of Technology, 80-233 Gdańsk, Poland

Jarosław Chojnacki – Department of Inorganic Chemistry, Faculty of Chemistry, Gdańsk University of Technology, 80-233 Gdańsk, Poland

Complete contact information is available at:

<https://pubs.acs.org/10.1021/acs.inorgchem.0c00435>

## Notes

The authors declare no competing financial interest.

## ■ ACKNOWLEDGMENTS

R.G. and N.S. thank the National Science Centre NCN, Poland (Grant 2016/21/B/ST5/03088), for their financial support and the TASK Computational Center for access to computational resources.

## ■ REFERENCES

- (1) Légaré, M. A.; Pranckevicius, C.; Braunschweig, H. Metal-lomimetic Chemistry of Boron. *Chem. Rev.* **2019**, *119* (14), 8231–8261.
- (2) Power, P. P. Main-Group Elements as Transition Metals. *Nature* **2010**, *463* (7278), 171–177.
- (3) Severin, K. Synthetic Chemistry with Nitrous Oxide. *Chem. Soc. Rev.* **2015**, *44* (17), 6375–6386.
- (4) Otten, E.; Neu, R. C.; Stephan, D. W. Complexation of Nitrous Oxide by Frustrated Lewis Pairs. *J. Am. Chem. Soc.* **2009**, *131* (29), 9918–9919.
- (5) Neu, R. C.; Otten, E.; Lough, A.; Stephan, D. W. The Synthesis and Exchange Chemistry of Frustrated Lewis Pair-Nitrous Oxide Complexes. *Chem. Sci.* **2011**, *2* (1), 170–176.
- (6) Mo, Z.; Kolychev, E. L.; Rit, A.; Campos, J.; Niu, H.; Aldridge, S. Facile Reversibility by Design: Tuning Small Molecule Capture and Activation by Single Component Frustrated Lewis Pairs. *J. Am. Chem. Soc.* **2015**, *137* (38), 12227–12230.
- (7) Tskhovrebov, A. G.; Solari, E.; Wodrich, M. D.; Scopelliti, R.; Severin, K. Covalent Capture of Nitrous Oxide by N-Heterocyclic Carbenes. *Angew. Chem., Int. Ed.* **2012**, *51* (1), 232–234.
- (8) Tskhovrebov, A. G.; Vuichoud, B.; Solari, E.; Scopelliti, R.; Severin, K. Adducts of Nitrous Oxide and N-Heterocyclic Carbenes: Syntheses, Structures, and Reactivity. *J. Am. Chem. Soc.* **2013**, *135* (25), 9486–9492.
- (9) Staudinger, H.; Hauser, E. Über Neue Organische Phosphorverbindungen IV Phosphinimine. *Helv. Chim. Acta* **1921**, *4* (1), 861–886.
- (10) Woolven, H.; González-Rodríguez, C.; Marco, I.; Thompson, A. L.; Willis, M. C. DABCO- Bis (Sulfur Dioxide), DABSO, as a Convenient Source of Sulfur Dioxide for Organic Synthesis: Utility in Sulfonamide and Sulfamide Preparation. *Org. Lett.* **2011**, *13* (18), 4876–4878.
- (11) Smith, B. C.; Smith, G. H. 1028. Sulphur Dioxide. Part II. Reactions of Tertiary Phosphines with Sulphur Dioxide. *J. Chem. Soc.* **1965**, 5516.
- (12) Buß, F.; Roterig, P.; Mück-Lichtenfeld, C.; Dielmann, F. Crystalline, Room-Temperature Stable Phosphine-SO<sub>2</sub> Adducts: Generation of Sulfur Monoxide from Sulfur Dioxide. *Dalton Trans.* **2018**, *47* (31), 10420–10424.
- (13) Aders, N.; Keweloh, L.; Pleschka, D.; Hepp, A.; Layh, M.; Rogel, F.; Uhl, W. P-H Functionalized Al/P-Based Frustrated Lewis Pairs in Dipolar Activation and Hydrophosphination: Reactions with CO<sub>2</sub> and SO<sub>2</sub>. *Organometallics* **2019**, *38* (14), 2839–2852.
- (14) Adenot, A.; von Wolff, N.; Lefevre, G.; Berthet, J. C.; Thuéry, P.; Cantat, T. Activation of SO<sub>2</sub> by N/Si- and N/B Frustrated Lewis Pairs: Experimental and Theoretical Comparison with CO<sub>2</sub> Activation. *Chem. - Eur. J.* **2019**, *25* (34), 8118–8126.
- (15) Sajid, M.; Klose, A.; Birkmann, B.; Liang, L.; Schirmer, B.; Wiegand, T.; Eckert, H.; Lough, A. J.; Fröhlich, R.; Daniliuc, C. G.; Grimme, S.; Stephan, D. W.; Kehr, G.; Erker, G. Reactions of Phosphorus/Boron Frustrated Lewis Pairs with SO<sub>2</sub>. *Chem. Sci.* **2013**, *4* (1), 213–219.
- (16) Lavigne, F.; Maerten, E.; Alcaraz, G.; Branchadell, V.; Saffon-Merceron, N.; Baceiredo, A. Activation of CO<sub>2</sub> and SO<sub>2</sub> by Boryl(Phosphino)Carbenes. *Angew. Chem., Int. Ed.* **2012**, *51* (10), 2489–2491.

(17) Szykiewicz, N.; Ponikiewski, Ł.; Grubba, R. Symmetrical and Unsymmetrical Diphosphanes with Diversified Alkyl, Aryl and Amino Substituents. *Dalton Trans.* **2018**, 47 (47), 16885–16894.

(18) Szykiewicz, N.; Ponikiewski, L.; Grubba, R. Diphosphination of CO<sub>2</sub> and CS<sub>2</sub> Mediated by Frustrated Lewis Pairs-Catalytic Route to Phosphanyl Derivatives of Formic and Dithioformic Acid. *Chem. Commun.* **2019**, 55 (20), 2928–2931.

(19) Szykiewicz, N.; Ordyszewska, A.; Chojnacki, J.; Grubba, R. Diaminophosphinoboranes: Effective Reagents for Phosphinoboration of CO<sub>2</sub>. *RSC Adv.* **2019**, 9 (48), 27749–27753.

(20) Ordyszewska, A.; Szykiewicz, N.; Perzanowski, E.; Chojnacki, J.; Wiśniewska, A.; Grubba, R. Structural and Spectroscopic Analysis of a New Family of Monomeric Diphosphinoboranes. *Dalton Trans.* **2019**, 48 (33), 12482–12495.

(21) Bailey, J. A.; Pringle, P. G. Monomeric Phosphinoboranes. *Coord. Chem. Rev.* **2015**, 297–298, 77–90.

(22) Bailey, J. A.; Sparkes, H. A.; Pringle, P. G. Single Oxygen-Atom Insertion into p-b Bonds: On- and off-Metal Transformation of a Borylphosphine into a Borylphosphinite. *Chem. - Eur. J.* **2015**, 21 (14), 5360–5363.

(23) Pyykkö, P.; Atsumi, M. Molecular Single-Bond Covalent Radii for Elements 1–118. *Chem. - Eur. J.* **2009**, 15 (1), 186–197.

(24) Wang, Y.; Li, Z. H.; Wang, H. Synthesis of an Oxygen-Linked Geminal Frustrated Lewis Pair and Its Application in Small Molecule Activation. *RSC Adv.* **2018**, 8 (46), 26271–26276.

(25) Zhu, D.; Qu, Z.; Stephan, D. W. Addition Reactions and Diazomethane Capture by the Intramolecular P-O-B FLP: tBu<sub>2</sub>POBcat. *Dalton Trans.* **2020**, 49, 901.

(26) Shieh, M.; Ho, C. H.; Sheu, W. S.; Chen, H. W. Selective Insertion of Oxygen and Selenium into an Electron-Precise Aramagnetic Selenium-Manganese Carbonyl Cluster [Se<sub>6</sub>Mn<sub>6</sub>(CO)<sub>18</sub>]<sup>4-</sup>. *J. Am. Chem. Soc.* **2010**, 132 (12), 4032–4033.

(27) Cristóbal, C.; Álvarez, E.; Paneque, M.; Poveda, M. L. Facile Oxygen Atom Insertion into Unactivated C(Sp<sup>3</sup>)-C(Sp<sup>2</sup>) Single Bonds in Reactions of Iridium(III) Complexes with O<sub>2</sub>. *Organometallics* **2013**, 32 (2), 714–717.

(28) Leisch, H.; Morley, K.; Lau, P. C. K. Baeyer-Villiger Monoxygenases: More than Just Green Chemistry. *Chem. Rev.* **2011**, 111 (7), 4165–4222.

(29) Nöth, H.; Schrägle, W. Beiträge Zur Chemie Des Bors, XXX. Zur Kenntnis von Monomerem Bis(Dimethylamino)-Diäthylphosphino-Boran. *Chem. Ber.* **1964**, 97 (8), 2218–2229.

(30) Pyykkö, P.; Atsumi, M. Molecular Double-Bond Covalent Radii for Elements Li-E112. *Chem. - Eur. J.* **2009**, 15 (46), 12770–12779.

(31) Bertini, F.; Lyaskovskyy, V.; Timmer, B. J. J.; de Kanter, F. J. J.; Lutz, M.; Ehlers, A. W.; Slootweg, J. C.; Lammertsma, K. Preorganized Frustrated Lewis Pairs. *J. Am. Chem. Soc.* **2012**, 134 (1), 201–204.

(32) Habraken, E. R. M.; Mens, L. C.; Nieger, M.; Lutz, M.; Ehlers, A. W.; Slootweg, J. C. Reactivity of the Geminal Phosphinoborane tBu<sub>2</sub>PCH<sub>2</sub>BPh<sub>2</sub> towards Alkynes, Nitriles, and Nitrilium Triflates. *Dalton Trans.* **2017**, 46 (36), 12284–12292.

(33) Corbridge, D. E. C. *Phosphorus: Chemistry, Biochemistry and Technology*, 6th ed.; CRC Press, 2013.

(34) Christiansen, A.; Li, C.; Garland, M.; Selent, D.; Ludwig, R.; Spannenberg, A.; Baumann, W.; Franke, R.; Börner, A. On the Tautomerism of Secondary Phosphane Oxides. *Eur. J. Org. Chem.* **2010**, 2010 (14), 2733–2741.